ISSN 1561-8889. Космічна наука і технологія. 2010. Т. 16. № 1. С. 46–54.

UDC 533.951

D. Yu. Klimushkin, P. N. Mager, N. A. Zolotukhina
Institute of Solar-Terrestrial Physics Russian Academy of Sciences, Siberian Branch, Irkutsk, Russia

SPATIO-TEMPORAL STRUCTURE OF POLOIDAL ALFVÉN WAVES IN THE MAGNETOSPHERE

This paper overviews some recent studies of spatio-temporal structure of poloidal (high-m) Alfvén waves (Pc4—5) in the magnetosphere, with taking into account finite field line curvature and plasma pressure. The effects of finite pressure plasma are especially essential near the magnetospheric equator, where an opaque region for Alfvén waves can be formed. This region is bounded by two turning points which restrain penetration of the wave energy far from the ionosphere, and an Alfvén resonator appears on a part of the field line adjacent to the ionosphere. Due to this effect the ULF pulsations in the Northern and Southern hemispheres can be non-conjugated. Another result is a peculiar field-aligned structure of the wave magnetic field: its fundamental harmonic must have three nodes, rather than one node as with cold plasma. The transverse structure of the wave is determined by the excitation mechanism. It is supposed in the report that wave is emitted by an alternating current created by the drifting particle cloud or ring current inhomogeneity. It is shown that the wave appears in some azimuthal location simultaneously with the particle cloud arrival at the same spot. The wave propagate westward, in the direction of the proton drift. The expected properties of the wave (amplitude, polarization, hodogram) are close to the observed properties of poloidal ULF pulsations.

INTRODUCTION

Among ultra low-frequency oscillations in the Earth's magnetosphere, the azimuthally small-scale Alfvén waves are distinguished, i. e., the waves with large azimuthal wave numbers $m>>1$. These waves usually have poloidal polarization i. e., field lines oscillate in radial direction. Recently these waves were studied with the multi-satellite CLUSTER mission [2, 15] and SuperDARN radars [17]. Theoretical studies of such waves are performed on the basis of magnetosphere models with the field lines curvature, two-dimensional inhomogeneity of the plasma and the magnetic field, the plasma finite pressure are taken into account.

Leonovich and Mazur [8] showed that in a curved magnetic field the high-m monochromatic Alfvén waves generally propagate across magnetic shells. However, it was found that the mode structure is very sensitive to the excitation process. For example, if the wave is excited by a impulsive source, the localization region can be a whole magnetosphere, with a wave polarization changing in time [6, 9]. Thus, in order to obtain results that can be compared with the experiments, one should elaborate theory of the realistic wave generation mechanism. There are some hints that these waves are generated by substorm injected particles drifting in the magnetosphere: there are statistical relations between high-m pulsations and ring current intensifications [1], and observations of events when the waves appeared in some azimuthal location simultaneously with a cloud of substorm injected protons [16]. A realistic generation mechanism was suggested by Guglielmi and Zolotukhina [4]: an excitation by a moving cloud of substorm injected particles by means of its alternating current. An analytical theory of the spatio-temporal evolution of the wave field generated by this mechanism in a curved magnetic field was developed by Mager and Klimushkin [10]. In this paper we are going to present an easy to grasp semi-qualitative version of this theory, along with some experimental arguments it its favour.

Besides, the field aligned structure of the high-m waves in the magnetosphere was not examined in full detail. Implicitly, it is commonly assumed that this structure has a typical scale of about the field line length between the conjugate ionospheres, being a sort of sinus function. However, at high latitudes where the magnetic field lines are essentially non-dipole, a field aligned structure can be different, which can significantly change the structure [13]. In this

paper we are going to examine a field-aligned structure of Alfvén waves taking into account the plasma inhomogeneity across magnetic shells and in the direction along an external magnetic field, the field line curvature, and finite plasma pressure.

PRINCIPAL EQUATIONS

Here we present the basic equations describing poloidal Alfvén waves in a finite pressure plasma immersed into a curved magnetic field. Let us introduce an orthogonal curvilinear coordinate system $\{x^1, x^2, x^3\}$, in which the field lines play the role of coordinate lines x^3, the stream lines are coordinate lines x^2, and the surfaces of constant pressure (magnetic shells) are coordinate surfaces $x^1 = \text{const}$. The coordinates x^1 and x^2 represent the radial and azimuthal coordinates; the parameter L and azimuthal angle φ, respectively, can be used to represent them. The physical length along a field line is expressed in terms of an increment of the corresponding coordinate as $dl_P = \sqrt{g_3}dx^3$, where g_3 is the component of the metric tensor, and $\sqrt{g_3}$ is the Lamé coefficient. Similarly, for the transverse direction one has $dl_1 = \sqrt{g_1}dx^1$, and $dl_2 = \sqrt{g_2}dx^2$. The determinant of the metric tensor is $g = g_1 g_2 g_3$.

We shall consider the magnetosphere within the axially symmetric approximation. In this case all equilibrium quantities (plasma pressure P_0, density ρ_0, and the magnetic field B_0) will be independent of the azimuthal coordinate. Plasma equilibrium in the magnetic field is described by the relation:

$$\nabla P_0 = (4\pi)^{-1}\mathbf{J}_0 \times \mathbf{B}_0. \qquad (1)$$

Here we have designated

$$\mathbf{J}_0 \equiv \nabla \times \mathbf{B}_0 = \frac{4\pi}{c}\mathbf{j}_\perp, \qquad (2)$$

where $\mathbf{j}_\perp$ is the current flowing through the magnetosphere across field lines.

The MHD wave of frequency ω, which propagates in hot plasma, is described by the equation [5]:

$$-\rho_0\omega^2\xi = \nabla(\xi\cdot\nabla P_0 + \gamma P_0\nabla\cdot\xi) + \frac{1}{4\pi}\mathbf{J}_0\times[\nabla\times[\xi\times\mathbf{B}_0]] -$$

$$-\frac{1}{4\pi}\mathbf{B}_0\times[\nabla\times\nabla\times[\xi\times\mathbf{B}_0]], \qquad (3)$$

where ξ is the displacement vector of plasma from the equilibrium position, and γ is the adiabatic index. The transverse component of the displacement vector may be expressed in terms of the wave's electric field $\mathbf{E}$:

$$\xi_\perp = -\frac{ic}{\omega}\frac{\mathbf{B}_0\times\mathbf{E}}{B_0^2}. \qquad (4)$$

Note that $\mathbf{E}\perp\mathbf{B}_0$ because of perfect plasma conductivity.

Within the approximation $m >> 1$, the electric field of the MHD wave may be represented as

$$\mathbf{E} = -\nabla_\perp\Phi. \qquad (5)$$

From equation (3), by using the relations (4), (5), it is possible to obtain the equation describing the Alfvén wave with $m >> 1$, propagating in a plasma with small but finite pressure [7]:

$$\left[m^2\hat{L}_P(\omega) - \partial_1\hat{L}_T(\omega)\partial_1\right]\Phi = 0. \qquad (6)$$

Following notation are introduced here: the operator of the toroidal mode

$$\hat{L}_T(\omega) = \partial_3\frac{g_2}{\sqrt{g}}\partial_3 + \frac{\sqrt{g}}{g_1}\frac{\omega^2}{A^2} \qquad (7)$$

(here $A = B_0/\sqrt{4\pi\rho}$ is the Alfvén velocity), and the operator of the poloidal mode

$$\hat{L}_P(\omega) = \partial_3\frac{g_1}{\sqrt{g}}\partial_3 + \frac{\sqrt{g}}{g_2}\left(\frac{\omega^2}{A^2} + \eta\right). \qquad (8)$$

Here

$$\eta = -2K\left(\frac{4\pi}{c}\frac{j_\perp}{B} + K\gamma\beta\right),$$

K is the local curvature of a field line, and γ is the adiabatic index.

For the ideally conducting ionosphere, the boundary conditions for the Φ-function («potential») are written as

$$\Phi\big|_{\pm l_I} = 0, \qquad (9)$$

where $\pm l_I$ denotes the points of the intersection of a field line with the ionosphere.

FIELD-ALIGNED STRUCTURE

It is obvious that when

$$\left|\frac{\partial\Phi}{\partial l_2}\right| >> \left|\frac{\partial\Phi}{\partial l_1}\right| \qquad (10)$$

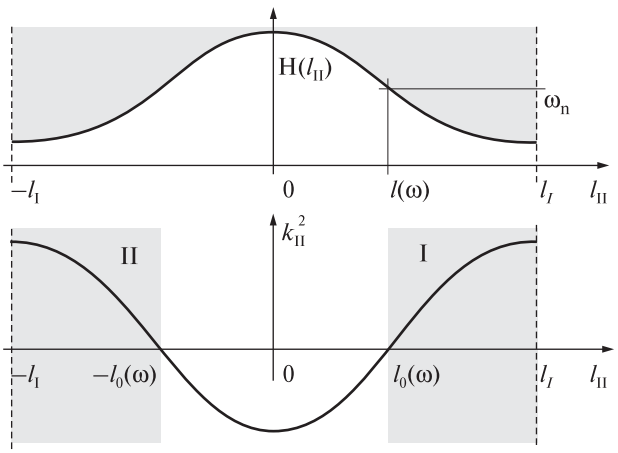

Fig. 1. Sketch demonstrating the dependence of H (top) and k_P^2 (bottom) on l_P and showing probable locations of the transparent and opaque regions. Here $\pm l_0$ are the turning points for a harmonic with eigenfrequency ω_n, $\pm l_I$ are the intersection points of a field line with the ionosphere. The shaded areas I and II correspond to the transparent regions.

the structure of the wave is determined by the poloidal operator; the necessary condition is a large value of the azimuthal wave number ($m >> 1$). Then, the equation determining the field-aligned structure of the poloidal mode is written as

$$\widehat{L}_P(\omega)\Phi = 0. \qquad (11)$$

Let us change the field-aligned variable to ξ determined as

$$d\xi = \frac{\sqrt{g}}{g_1} dx^3.$$

As a result, Eq. (11) can be presented in the form of the Schrödinger equation:

$$\frac{\partial^2}{\partial \xi^2}\Phi + \frac{g_1}{g_2}\frac{\omega^2 - H(\xi)}{A^2}\Phi = 0, \qquad (12)$$

where the term

$$H(\xi) = -A^2\eta = A^2 2K\left(\frac{4\pi}{c}\frac{j_\perp}{B} + K\gamma\beta\right) \qquad (13)$$

is often called the ballooning term.

For heuristic purposes, Eq. (12) will be solved first in the WKB approximation. The resulting field-aligned component of the wave vector is determined from the expression:

$$k_P^2(\xi) = \frac{\omega^2 - H(\xi)}{A^2}. \qquad (14)$$

In a cold plasma, when $H = 0$, an Alfvén wave has no turning point, that is $k_P^2 > 0$ everywhere. Thus the entire field line between the conjugate ionospheres is transparent for the Alfvén wave and the oscillation has a familiar sinusoidal structure. Let us denote the harmonic wave number N as a number of nodes plus 1 (that is, the fundamental harmonic has $N = 1$).

In a finite pressure plasma, the sign and magnitude of the ballooning term in (12) determines the field-aligned structure of the wave disturbance. An interesting effect occurs under the outward gradient of pressure, $\partial P/\partial x^1 > 0$. Let us find the region along the field line where the function $H(\xi)$ has its maximum. Usually, the second term in (13) dominates, thus H varies along the parallel coordinate as $H \propto K^2\rho^{-1}$, where ρ is the plasma density. The plasma pressure is to be constant along the field line, whereas the field line curvature K and inverse density ρ^{-1} both peak near the equator. Therefore, the function $H(\xi)$ has a maximum at the equator (Fig. 1) and $H > 0$.

As it follows from Eq. (14), in this case the function $k_P^2(\xi)$ can change its sign along the field line. The point l_0, where $k_P^2(l_0) = 0$, is the turning point for a poloidal Alfvén wave. The region where $k_P^2 < 0$, is an opaque region, where the wave becomes evanescent, and the region where $k_P^2 > 0$ is transparent for waves.

When H has a maximum at the magnetospheric equator, which is usually the case, the opaque region is located in the vicinity of the top of a field line. Thus, two sub-resonators (regions I and II in Fig. 1) are formed, bounded by the ionosphere and the turning point near the equator, $\pm l_0$.

The structure of the wave potential Φ_1 for the fundamental mode must be most deformed in comparison with the cold plasma case, since the opaque region is largest and «deepest» for it. Furthermore, in the magnetosphere the opaque region may not exist for higher harmonics. In a cold plasma, the amplitude of the electric field of the fundamental harmonic ($N = 0$) has a maximum at the equator. In a finite pressure plasma with an opaque region near the top of a field line, it has a minimum at the equator and

two maxima in both hemispheres, that is a total of three extremes. The wave transverse magnetic field b is determined by the field-aligned derivative of potential Φ as

$$b_1 \propto \frac{1}{\sqrt{g_2}} \frac{\partial}{\partial l_P} \Phi.$$

Therefore, the magnetic field of the fundamental harmonic must have three nodes, rather than one node as in a cold plasma. The magnetic field of the second harmonic must have only two nodes, just like in the $\beta = 0$ case.

Since the WKB approximation cannot give the quantitative results for the fundamental modes, a numerical solution of the wave equation (11) must be performed. The results of this modeling completely confirm those of the WKB analysis, described above (Fig. 2), equatorial including gap of the wave electric field and three node structure of the magnetic field. For more details of the numerical calculations, see [12].

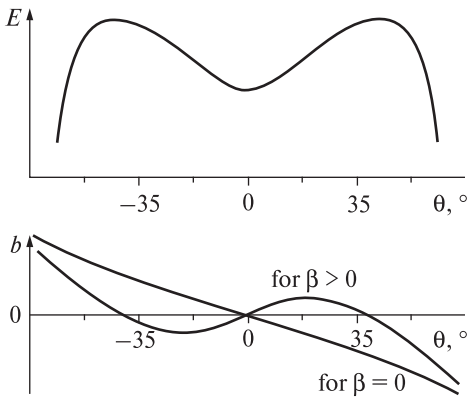

Fig. 2. The field-aligned structure of the fundamental harmonic at $L = 6$ shell. Here E and b are the wave electric and magnetic fields, respectively, and θ is the geomagnetic latitude. For the wave magnetic field, the structure for $\beta = 0$ and $\beta > 0$ cases is shown. The ratio of equatorail plasma to magnetic pressure is $\beta_{eq} = 0.8$

TRANSVERSE STRUCTURE

Theory. The generation of the Alfvén wave by a cloud of substorm injected particles in a curved magnetic field was studied by Mager and Klimushkin [10] in terms of the stationary phase method. But the main features of the spatio-temporal structure of the wave field can be elucidated in a rather simple qualitative way.

Let us consider a cloud of particles injected into the axially-symmetric magnetosphere at some time instant $t = 0$. This cloud can be considered as an impulse propagating from one location on the azimuthal coordinate to another at drift angular velocity $\omega_d(x)$.

Wave excitation by a sudden impulse in the entire magnetosphere is well studied theoretically [6, 9]. In this case, the azimuthal wave number m may be prescribed arbitrarily. Each field line oscillates with its own eigenfrequency ω, which depends on the radial coordinate x (the coordinate across magnetic shells). Hence, the electric field of the wave is determined by the expression:

$$E_{x,y} = | E_{x,y} | e^{-i\omega(x)t + im\varphi}, \qquad (15)$$

where φ is the azimuthal angle (it is equivalent to the x^2 coordinate) and y denotes the azimuthal coordinate, which can be defined as $y = \varphi L$. In the course of the evolution the wave structure becomes smaller-scale in the radial direction due to the phase mixing, and an initially poloidally polarized wave transforms into a toroidal one.

For the azimuthally drifting source, the m number is determined by the generation mechanism. In the reference system of the source, the phase just behind the source must be constant, thus the Doppler-shifted wave frequency $\omega^* = \omega - m\omega_d$ must be zero. Hence, we obtain the expression for the m-number:

$$m = \frac{\omega(x^1)}{\omega_d(x^1)}. \qquad (16)$$

Note that this value depend on the radial coordinate. Hence, eq. (15) is replaced by

$$E = \Theta(\omega_d t - \varphi) | E | e^{i\Psi}. \qquad (17)$$

Here Ψ is the wave phase determined as:

$$\Psi = -\omega(x)t + \frac{\omega(x^1)}{\omega_d(x^1)}\varphi. \qquad (18)$$

The Heaviside step function $\Theta(\omega_d t - \varphi)$ indicates that the wave appears in some azimuthal location

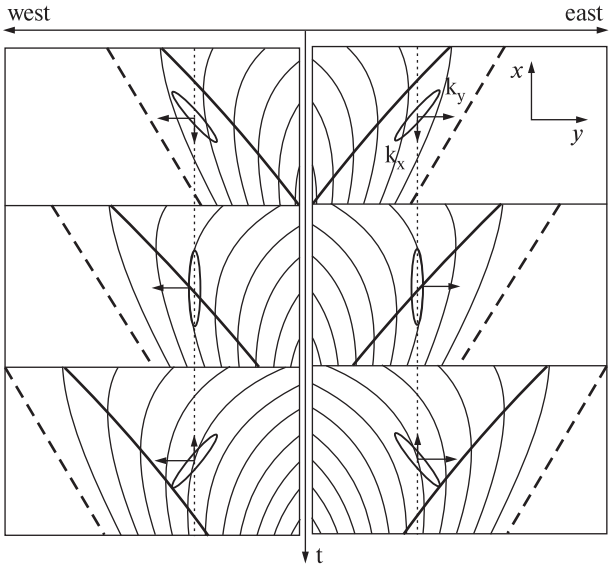

Fig. 3. Polarization ellipses of the wave excited by the moving cloud at different time instants. Dashed lines represent the drifting source. The bold line corresponds to $k_x = 0$ (purely poloidal polarization of the wave). The right and left parts of the figure correspond to electrons and ions, respectively. Thin lines represent the lines of constant phase

simultaneously with the particle cloud arrival in the same spot because the energy of the Alfvén wave almost does not propagate transverse to the field lines: the wave can be viewed as to be carried by the cloud.

Let us describe the main features of the solution obtained.

Azimuthal wave structure. The wave frequency is fully determined by the radial coordinate and does not depend on the nature of the source. So, if two clouds are drifting in opposite azimuthal directions, they must generate waves with the same frequencies determined by the eigenfrequency on this magnetic surface: $\omega = \omega(L)$. But the azimuthal wave number depends on the particle energy because it is defined through the equality (16) and the drift frequency depends on the particle energy as

$$\omega_d \approx 8 \cdot 10^{-3} \varepsilon L, \qquad (19)$$

where ω_d, L, and ε are measured in degrees per minute, Earth's radii, and keV, respectively [14]. So, one can expect different $|m|$ values for the wave generated by electrons and ions.

Radial structure and phase motion. The radial k_x and azimuthal k_y components of the wave vector are defined through the phase as $k_x = \partial\Psi/\partial x$ and $k_y = \partial\Psi/\partial y$. Here the azimuthal component is $k_y = m/L$. Its sign is determined by the direction of the drift. It points westward (eastward) if the wave is excited by ions (electrons).

Let $t_0 = \varphi/\omega_d$ be a time instant when the source reaches the point with a given azimuthal coordinate φ. The Heaviside function $\Theta(\omega_d t - \varphi)$ in the Eq. (17) shows that if $t < t_0$, the wave field is absent.

The wave vector radial component is determined as

$$k_x = \Psi' = -\left(\frac{\omega}{\omega_d}\right)(\omega_d t - \varphi) - \omega t \frac{\omega_{d'}}{\omega_d} \qquad (20)$$

(prime means the radial derivative, $\partial/\partial l_1$). Its sign depends on the drift velocity profile and varies with space and time. Let us consider the most interesting case when the drift frequency increases with the radial coordinate. Since in the most part of the magnetosphere the Alfvén eigenfrequency decreases with L, $\omega' < 0$, then the first right-hand side term of the previous equation is positive when $t > t_0$ and grows with time, but the second one is always negative. Thus, there is also another special time instant,

$$t_1 = \varphi \frac{(\omega/\omega_d)'}{\omega'}.$$

It is clearly seen that just after moment of the source passing the point with given azimuthal coordinate ($t_0 = \varphi/\omega_d$) till t_1, the wave vector radial component is negative, $k_x < 0$. It means the equatorward phase propagation in projection onto the ionosphere along the field lines. At the moment t_1 the radial component changes its sign and becomes positive.

Wave polarization. The Alfvén wave magnetic field oscillates transverse to the perpendicular wave vector, $\mathbf{B}_\perp \cdot \mathbf{k}_\perp = 0$, hence the ratio of the radial and azimuthal magnetic field components is

$$\frac{B_x}{B_y} = -\frac{k_y}{k_x}. \qquad (21)$$

Since both B_x and B_y components are presented in the wave field, the mode has a mixed polarization (intermediate between toroidal and poloidal). At the moment t_1 this value becomes zero, $k_x = 0$. It is the moment when the mode is purely poloidal for the given location. When $t > t_1$, the wave vector radial

component becomes positive. In the course of time, k_x grows, which means that the mode trasforms from poloidal to toroidal. A reason for this transformation is the phase mixing. Indeed, for $t >> t_1$, the first term in Eq. (18) is much larger, than the second one, and k_x is determined by the derivative of the first term (as in Eq. 15), that is, it grows with time as $k_x \approx -\omega' t$.

The corresponding polarization ellipse of the wave is depicted in Fig. 3. It must be noted that the wave is approximately linearly polarized because in the WKB approximation both radial and azimuthal magnetic field components have the same phase. The most interesting feature of these graphs is the change of the polarization ellipse orientation due to the k_x sign change. At the beginning, the ellipse is inclined to the x axis (mixed wave polarization), then it is directed along this axis (pure poloidal polarization), then it is inclined in the opposite direction (mixed polarization again).

A simple qualitative explanation of this wave polarization change can be given. Let us plot the lines of constant phase in the $x - \varphi$ plane (see Fig. 3). Consider the wave generated by protons. The whole pattern in Fig. 3 is shifting in the right-hand side direction. Just nearby the source they go almost parallel to the source. Due to the assumed increase of particle drift velocity with distance from the Earth, the source stretches into the strip at an acute angle to the lines $x = const$ (the angle is measured counter-clockwise), which leads to inward phase motion and negative k_x. In the vicinity of the source, the wave can be considered as a plane wave (the line of the constant phase go almost parallel to each other), hence the phase difference between two nearby points with the same φ value is determined as $\Delta\Psi \approx k_x(x_2 - x_1)$. If $x_2 > x_1$ this difference is negative. But after the source has passed the point with given φ coordinate, each field line becomes oscillating with its own frequency decreasing with the radial coordinate (phase mixing), and the phase difference becomes $\Delta\Psi \approx k_x(x_2 - x_1) - -(\Omega(x_2) - \Omega(x_1))t$. Here $\Omega(x_2) < \Omega(x_1)$, thus $\Delta\Psi$ decreases with time, and at some instant changes its sign. So, it is phase mixing which is responsible for the change of the sign of the radial phase velocity and corresponding change of the wave polarization.

Comparison with the experiments. If the drift velocity grows with the radial coordinate, the particle

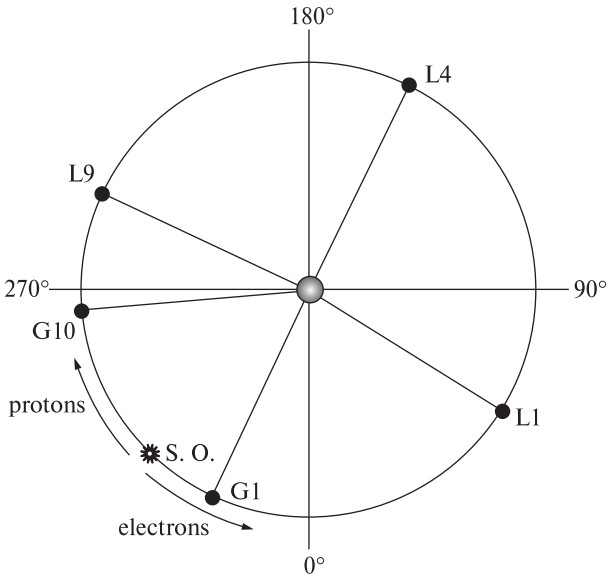

Fig. 4. The position of the substorm onset and the satellites for the moments of observations of the events

cloud is stretched into spiral in the equatorial plane. This leads to inward phase motion and negative value of the wave vector radial component or, being projected onto the ionosphere, to the equatorward phase propagation. This still unexplained feature of the high-m waves was often observed with radars (see, e.g., [17]). As we see, it has a simple explanation in terms of theory, considered here [11].

Yet another validation of this theory is given by substorm related Pc5 event considered in detail by Zolotukhina et al. (2008). The substorm happened on September 17, 2000, with the onset at 03:20:25 UT at the geographical longitude $\lambda = 266^\circ$ [3]. Geostationary satellites GOES 8 and 10 have the geographical longitudes $\lambda = 285^\circ$ (GOES 8) and $\lambda = 225^\circ$ (GOES 10), thus the onset took place between the satellites (Fig. 4).

Shortly after the onset, the satellites registered Pc5 variations of magnetic field: immediately after the onset at GOES 8 and 12—14 min after the onset at GOES 10. The periods of oscillations observed by both satellites were almost the same: at 220 s (GOES 8) and 230 s (GOES 10).

Satellites' magnetic data were transformed into the mean-field-aligned coordinate system: the x and y

coordinates are directed outward (radial coordinate) and eastward (azimuthal coordinate), and z coordinate is directed along the averaged magnetic field. Hence, the transformed $B_x(t)$, $B_y(t)$, and $B_z(t)$ variations approximately describe the poloidal, toroidal and field aligned components of magnetic field vector **B**, respectively. It is significant that in B_z auto-spectra from GOES 8 and GOES 10 there were no spectral maxima at the same periods as in transverse components B_x, B_y. Thus we believe that in the case under study the Pc5 were transverse magnetic field oscillations.

After GOES 8 and 10 observed the magnetic fluctuations, the LANL satellites detected an increase of the particle fluxes (positions of the satellites are depicted in Fig. 3). West of the onset, the increase was in proton flux J_p: first it was registered by the LANL 9 satellite located west of the onset ($\Delta\lambda = 71^\circ$; here and below the $\Delta\lambda$ values are positive/negative west/east of the substorm onset meridian) in Δt =18—25 minutes after the onset, then by LANL 4 ($\Delta\lambda = 162^\circ$, $\Delta t = 28$ to 47 min) and even later by LANL 1 ($\Delta\lambda = 258^\circ$, $\Delta t = 40$ to 70 minutes). An analogous picture was observed for electron flux J_e: first it was registered by LANL 1 ($\Delta\lambda = -102^\circ$, $\Delta t = 25$ to 50 min) then by LANL 4 ($\Delta\lambda = -198^\circ$, $\Delta t = 44$ to 66 min). With promotion in the east (LANL 9, 4, and 1) or west (LANL 1 and 4) direction, the flux growth rate was damping.

In the inhomogeneous geomagnetic field, particles of opposite charges drift in opposite directions: negative particles (electrons) drift eastward, and positive particles (ions) drift westward. This immediately provides an interpretation of the double event reported in the previous section: GOES 8 (located east of the substorm onset) detected waves generated by drifting electrons, and GOES 10 (west of the onset) detected waves generated by positive ions. Thus, we have a heuristic model of the event: substorm injected clouds of particles (with opposite charges) directly drive the waves. The waves observed by both GOES 10 and GOES 8 satellites have almost the same frequencies, which fits the theoretical expectations described above: being determined by the radial coordinate, the wave frequency should not depend on the nature of the source.

The proton cloud was drifting westward and had performed almost complete turn around the Earth. The damping of flux growth rate $\dot{J}_p$ in the course of the drift is a natural consequence of the cloud spreading, as is expected in the case of the injection localized in the azimuthal coordinate. With a knowledge of the LANL 9 angular distance (LANL 9 was the nearest satellite to GOES 10) from the point of the substorm onset, $\Delta\lambda = 71^\circ$, and the corresponding time lag Δt =18—25 min, it is possible to calculate the drift velocities of the particles comprised the leading front of the proton cloud: $\omega_d = 3^\circ$ to 4° per a minute. Thus, at the instant of GOES 10 magnetic observations, the proton cloud indeed was somewhere nearby this satellite. An interpretation of the Pc5 pulsations registered by GOES 8 satellite is similar, but here observed were the oscillations generated by the substorm injected electrons.

This conclusion is supported by the inspection of the hodograms of the pulsations registered by GOES 10 and GOES 8 satellites. These hodograms are depicted in Fig. 5 (200—250 s filtered magnetic field oscillations, the xy plane). It is clearly seen in this figure that the direction of the transverse magnetic field oscillations ($B_\perp$) changes with time. At GOES 8 $B_\perp$ rotates counterclockwise: $B_\perp$ oscillates along the $(+x,+y) \leftrightarrow (-x,-y)$ direction at the beginning, along the x axis at the midpoint, and along the line $(+x,-y) \leftrightarrow (-x,+y)$ at the end. The sign of $B_\perp$ rotation at GOES 10 is opposite to that at GOES 8: it rotates clockwise from the beginning to the end of the wave packet. Accordingly, the polarization of the waves detected by both satellites changes from mixed (between poloidal and toroidal) to poloidal, and then to mixed again.

As is seen from the comparison of Fig. 5 and 3, these are the very features expected from the theory. The hodograms of the wave detected by GOES 8 and 10 rotated counterclockwise and clockwise, respectively, as was expected for the waves generated by the clouds of electrons and ions, the polarization was linear and changes from mixed to poloidal to mixed again. This gives us additional hints for our interpretation.

It is possible to evaluate the energy of the particles responsible for the wave generation. The wave activity

at GOES 10 (located about 40° west of the place of the injection) started 12—14 min after the onset. Using Eq. (19), we get the energy of ions $\varepsilon \sim 60$ keV. The drift velocity ω_d from 3° to 4° per minute, calculated from the LANL 9 data ($L = 6.6 R_E$), corresponds to proton energy ε from 55 to 75 keV, which is quite close to the previous estimate (note that GOES 10 was situated about 30° east of LANL 9). At LANL 4 location ($\Delta\lambda = 162^\circ$ W), the drift velocity is $\omega_d \sim 3.4^\circ$/min to 5.8°/min, which corresponds to the energy from ε: 65 to 110 keV, and at LANL 1 location ($\Delta\lambda = 258^\circ$ W) the drift velocity is $\omega_d \sim 3.7^\circ$/min to 6.5°/min, and the energy is $\varepsilon \sim 70$ to 120 keV. It is evident that the energy of the protons, forming the cloud leading (western) front, gradually increases in the course of drift, which can be explained by the non-stationarity and azimuthal non-uniformity of the magnetosphere, as well as by the precipitations of the low energy particles into the ionosphere. Nonetheless, the rough coincidence of the estimates obtained from the GOES 10 and LANL 9 (nearest to GOES 10) data shows that it was a substorm injected westward drifting proton cloud, which was responsible for the generation of the waves seen in the GOES 10 data.

Unfortunately, the small angular distance between the place of the injection and the GOES 8 location together with the finite azimuthal size of the source and rather rough time resolution make impossible to perform an analogous estimation of the electron energy from the GOES 8 magnetic data and compare it with the LANL 1,4 results.

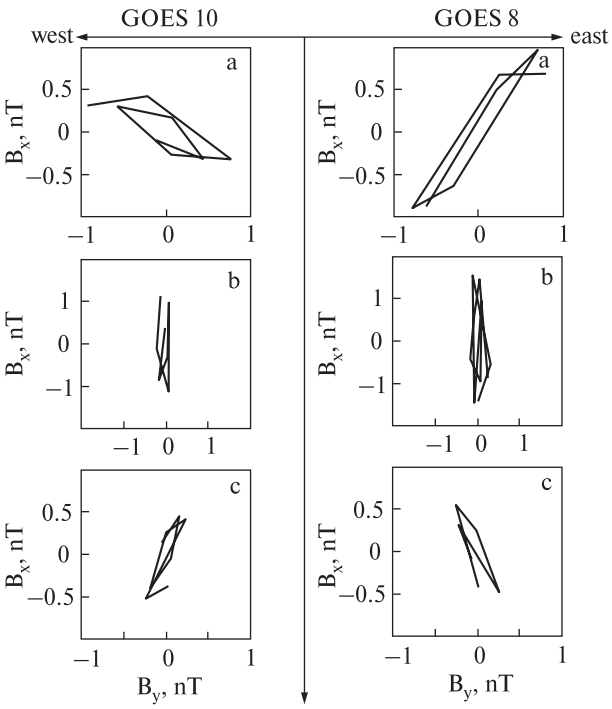

Fig. 5. The hodograms of the waves detected by GOES 10 (left) and GOES 8 (right) in the 200—250 s band

CONCLUSIONS

Ballooning term in the differential equation describing the field aligned structure of poloidal Alfvén waves in a finite pressure plasma, represent an effect of the finite-pressure plasma on the mode spatial structure. Under realistic conditions, it results in the occurrence of the opaque region in the vicinity of the equatorial plane of the magnetosphere. Consequently, the wave is composed of two weakly related parts adjacent to the ionosphere with a dip of an amplitude in the equatorial region. Due to this effect non-conjugate long-period (Pc4-5 and Pi2) pulsations may be observed, or oscillations with a peculiar field-aligned structure: the wave magnetic field of the fundamental harmonic must have three nodes, rather than one node as is the in cold plasma.

It is suggested that the poloidal Alfvén waves are generated by alternating current of substorm injected particles drifting in the magnetosphere in the azimuthal direction. If the drift velocity grows with the radial coordinate, the particle cloud is stretched into spiral in the equatorial plane. This leads to inward phase motion and negative value of the wave vector radial component or, being projected onto the ionosphere, to the equatorward phase propagation, often observed with radars.

This theory can also provide an interpretation of the event occured just after 17.09.2000 substorm onset: the satellites GOES 8 and 10 satellites registered Pc5 waves after the onset with the properties expected from the theory, namely double change of the polarization (mixed $\rightarrow$ poloidal $\rightarrow$ mixed), and change of the orientation of the polarization ellipse. It is possible that GOES 8 (located east of the substorm onset) detected the waves generated by drifting electrons,

and GOES 10 (west of the onset) detected the waves generated by positive ions. The estimated energy of the ions responsible for the wave generation is ~60 keV. This estimation is confirmed by the energetic particles data recorded by LANL satellites.

Acknowledgements. The work is supported by RFBR grant 07-05-00185, programs of Presidium of Russian Academy of Sciences no.16, OFN RAS no.16, and program no.9 of the Earth's sciences department of the Russian academy of sciences.

REFERENCES

1. *Anderson B. J., Potemra T. A., Zanetti L. J., et al.* Statistical correlation between Pc3—5 pulsations and solar wind/IMF parameters and geomagnetic indices // Physics of Space Plasmas: SPI Conference Proceedings and Reprint Series / Eds T. Chang, G. B. Crew,J. B. Jasperse. — Cambridge, Massachusetts: Scientific Publishers Inc., 1991. — Vol. 10. — P. 419—429,
2. *Eriksson P. T. I., Blomberg L. G., Walker A. D. M., et al.* Poloidal ULF oscillations in the dayside magnetosphere: a Cluster study // Ann. Geophys. — 2005. — **23**. — P. 2679—2686.
3. *Frey H. U., Mende S. B., Angelopoulos V., et al.* Substorm onset observations by IMAGE-FUV // J. Geophys. Res. — 2004. — **109**. — A10304, doi:10.1029/2004JA010607.
4. *Guglielmi A. V., Zolotukhina N. A.* Excitation of Alfvén oscillations of the magnetosphere by the asymmetric ring current // Issled. geomagn. aeron. i fiz. Solntsa. — 1980. — **50**. — P. 129—137 (in Russian).
5. *Kadomtsev B. B.* Hydromagnetic stability of plasma // Voprosy teorii plazmyed / Ed. by M. A. Leontovich. — Moskow: Gosatomizdat, 1963. — P. 132—176 (in Russian).
6. *Klimushkin D. Yu., Mager P. N.* The spatio-temporal structure of impulse-generated azimuthal small-scale Alfvén waves interacting with high-energy charged particles in the magnetosphere // Ann. Geophys. — 2004. — **22.** — P. 1053—1060.
7. *Klimushkin D. Yu., Mager P. N., Glassmeier K.-H.* Toroidal and poloidal Alfvén waves with arbitrary azimuthal wave numbers in a finite pressure plasma in the Earth's magnetosphere // Ann. Geophys. — 2004.— **22**. — P. 267—288.
8. *Leonovich A. S., Mazur V. A.* A theory of transverse small scale standing Alfvén waves in an axially symmetric magnetosphere // Planet. Space Sci. — 1993. — **41**. — P. 697—717.
9. *Leonovich A. S., Mazur V. A.* Standing Alfvén waves in an axisymmetric magnetosphere excited by a non-stationary source // Ann. Geophys. — 1998. — **16**. — P. 914—920.
10. *Mager P. N., Klimushkin D. Yu.* Alfvén ship waves: high-*m* ULF pulsations in the magnetosphere, generated by a moving plasma inhomogeneity // Ann. Geophys. — 2008. — **26**. — P. 1653—1663.
11. *Mager P. N., Klimushkin D. Yu., Ivchenko N.* On the equatorward phase propagation of high- *m* ULF pulsations observed by radars // J. Atmospheric and Solar-Terrestrial Phys. — 2009. — **71**. — P. 1677—1680.
12. *Mager P. N., Klimushkin D. Yu., Pilipenko V. A., et al.* Field-aligned structure of poloidal Alfvén waves in a finite pressure plasma // Ann. Geophys. — 2009. — **27**.
13. *Pilipenko V. A., Mazur N. G., Fedorov E. N., Engebretson M. J., et al.* Alfvén wave reflection in a curvilinear magnetic field and formation of Alfvénic resonators on open field lines // J. Geophys. Res. — 2005. — 110. — A10S05, doi:10.1029/2004JA010755.
14. *Roederer J. G.* Dynamics of geomagnetically trapped radiation. — New York: Springer-Verlag, 1970.
15. *Schäfer S., Glassmeier K.-H., Eriksson P. T. I., et al.* Spatio-temporal structure of a poloidal Alfven wave detected by Cluster adjacent to the dayside plasmapause // Ann. Geophys. — 2008. — **26**. — P. 1805—1817.
16. *Wright D. M., Yeoman T. K., Rae I. J., et al.* Ground-based and Polar spacecraft observations of a giant (Pg) pulsation and its associated source mechanism // J. Geophys. Res. — 2001. — **106**. — P. 10837—10852.
17. *Yeoman T. K., Wright D. M., Baddeley L. J.* Ionospheric sigatures of ULF waves: active radar techniques // Magnetospheric ULF waves: Synthensis and New Directions: Geophys. monograph ser. — 2006. — N 169. — P. 273—288. — 10.1029/169GM18.

Received October 1, 2009

Д. Ю. Климушкін, П. М. Магер, Н. О. Золотухіна

ПРОСТОРОВО-ЧАСОВА СТРУКТУРА ПОЛОЇДАЛЬНИХ АЛЬВЕНІВСЬКИХ ХВИЛЬ У МАГНІТОСФЕРІ